

Test rig for friction force measurements in pneumatic components and seals

*Original*

Test rig for friction force measurements in pneumatic components and seals / Belforte, Guido; MANUELLO BERTETTO, Andrea; Mazza, Luigi. - In: PROCEEDINGS OF THE INSTITUTION OF MECHANICAL ENGINEERS. PART J, JOURNAL OF ENGINEERING TRIBOLOGY. - ISSN 1350-6501. - STAMPA. - 227:1(2013), pp. 43-59.  
[10.1177/1350650112453522]

*Availability:*

This version is available at: 11583/2503094 since:

*Publisher:*

Sage publications

*Published*

DOI:10.1177/1350650112453522

*Terms of use:*

This article is made available under terms and conditions as specified in the corresponding bibliographic description in the repository

*Publisher copyright*

(Article begins on next page)

# **TEST RIG FOR FRICTION FORCE MEASUREMENTS IN PNEUMATIC COMPONENTS AND SEALS**

Guido Belforte, Andrea Manuello Bertetto, Luigi Mazza

## **ABSTRACT**

This article describes the design of a new test rig for measuring the friction force in pneumatic components and seals. The test rig was designed in order to measure both the overall friction force in a pneumatic cylinder or a valve as a whole, and the single contribution to friction force caused by the sliding seals. To this end, special fixtures and devices were designed and manufactured in order to measure the friction force in piston seals, rod seals and cartridge valve seals individually. Results of friction measurements carried out on pneumatic cylinders with similar characteristics but produced by different manufacturers are presented and compared. A test procedure and a methodology, in order to separate the contributions of the individual seals from the overall friction of the cylinders, is presented.

## **KEYWORDS**

Friction, seals, sealing systems, pneumatic actuators

## **INTRODUCTION**

Pneumatic cylinders are fundamental elements in factory automation and are used in many industrial devices, thanks to advantages including low cost, easy maintenance, good power density and easy assembly. As compressed air is available in almost

every industrial installation, pneumatic cylinders and valves have become competitive in many applications such as motion control of materials, gripper devices, robotics, industrial processes and the food processing industry. However, the friction force between seals and counterparts in relative sliding motion affects efficiency, reliability, stick-slip phenomenon and seal/counterface wear. In particular, seal malfunction as a result of high friction, low sealing capability, incorrect lubricating conditions or incorrect choice of seal material and geometry leads to lower system performance, higher operating costs and costly system maintenance. Conversely, reducing friction forces improves the performance and efficiency of pneumatic components and extends service life, thus making it possible to employ them in a wider range of industrial applications.

Friction in pneumatic actuators and valves has attracted considerable interest among researchers. Experimental analysis has demonstrated the importance of measuring pneumatic or hydraulic actuator friction as precisely as possible, taking all the physical parameters affecting the phenomenon into account. Methodologies have been developed that consider both dynamic friction force at a constant actuator velocity and dynamic friction force in unsteady motion.

The experimental methods proposed by Belforte et al. [1], Schroeder and Singh [2], Eschmann [3] and Ellman et al. [4] are based on measuring the overall friction force in pneumatic and hydraulic actuators at different constant velocity given time-invariant pressure differential across the piston. The test rigs were provided with a cylinder under test driven by a hydraulic cylinder, and a force sensor used to measure the force exchanged between the rods of the driving cylinder and the cylinder under test. Friction force was determined by means of the force sensor moving at the velocity of the rod; in this way, unfortunately, the force measurement is sensitive to

dynamic loads and inertial effects. In addition, the fact that the cylinder under test was driven by a hydraulic linear actuator made it impossible to carry out tests in the low speed range (below 20 mm/s). Kazama and Fujiwara [5], Belforte et al. [6] overcame these limitations by developing a method for measuring the friction force in double-acting pneumatic cylinders using a non-moving force transducer connected between the stationary portion of the cylinder and the test bench frame. The mobile portion of the cylinder was driven by a hydraulic or electric linear actuator. A linear air guideway supports the actuator under test to ensure that forces are correctly transmitted to the force transducer. These methods assess the overall friction force in pneumatic cylinders under different operating conditions without going into the details of the individual contributions to friction made by the sliding piston and rod seals.

To gain a better understanding of the friction phenomenon, several papers have dealt with single contributions to the overall actuator friction force, considering piston seal friction and rod seal friction individually. In particular Muller et al. [7, 8] develop experimental method for measuring friction and leakage in reciprocating seals for hydraulic cylinders. Belforte et al. [9, 10], Raparelli et al. [11] and Wassink et al. [12, 13] propose experimental methods for evaluating the effect of mounting tolerances, cylinder bore material, seal material properties, oil viscosity and temperature on pneumatic piston seal friction and on lip seals for hydraulic cylinder rods. In this last case not only friction but oil leakage is an important phenomenon; to this aim Haas et al. [14, 15] develop proper experimental set-up to evaluate leakage with reference to the film thickness on new and used sealing ring. The friction test results obtained made it possible to develop experimental models for calculating friction force in seals. Calvert et al. [16] and Belforte et al. [17] carried out experimental friction tests and

finite element analyses in order to redesign and optimise a seal cross-section geometry with the aim of improving tribological performance and reducing friction. The proposed methods and the tests that were carried out consider friction forces measured with seal sliding speeds in a single direction of motion. Unlike other investigations, Helduser and Muth [18] and Fujii [19] propose an indirect method of measuring friction in unsteady motion, and without using a force transducer. The friction force is thus determined by calculating inertial force from a measurement of the acceleration of the moving mass either made with an accelerometer or obtained from a derivative of a laser velocimeter signal.

This paper deals with the development of an experimental method and a test rig for measuring the friction force in whole pneumatic components and individual seals. The test rig will be presented together with the operating principle of the configurations developed for measuring the overall friction of complete pneumatic actuators and the friction force of individual piston seals, rod seals and pneumatic valve seals. For this purpose, special fixtures were designed and manufactured to reproduce the behaviour of a piston/bore system, a front head/rod system and a spool/cartridge system. The linear motion of the moving part (either a piston, a rod or a cartridge, depending on the seal type under test), is guided by special supports provided with air bearings in order to prevent any undesired additional friction and stick-slip phenomena and ensure precise measurement. This motion is produced by a linear electric cylinder in order to provide a larger low-velocity measurement range than would be possible with a conventional test bench driven by a hydraulic cylinder. Test rig architecture is designed so that dynamic and inertial loads have no influence; to this end, a load cell is placed between the body of the fixture and the test rig frame, while the fixture body is supported by a linear air bearing. Friction force

measurements on commercial double-acting pneumatic cylinders from different manufacturers will be presented. In particular, behaviour while varying fluid pressure seal geometry, rod velocity and direction of motion will be assessed. Analyzing the results for overall friction force on complete actuators, while allowing for the fact that friction is dependent on direction of motion, will make it possible to gain a better understanding of the behaviour of individual actuator seals.

## **EXPERIMENTAL SET-UP**

The test rig described herein was designed in order to measure the overall friction force on pneumatic cylinders as a whole and the friction force of individual piston seals, rod seals and pneumatic valve seals. The experimental apparatus is a modular system capable of performing different kinds of tests on different pneumatic cylinder types, geometries, sizes and individual sliding seal materials. Four different layouts were developed and equipped to perform the test indicated above, viz.: system layout 1, the basic test rig configuration used to measure overall friction force in a pneumatic cylinder considered as a whole, system layouts 2, 3 and 4 to measure the individual friction in piston seal, rod seal and valve seal respectively.

In particular layouts 2, 3 and 4 can be assembled by replacing some components in the basic configuration (layout 1).

### System layout 1.

A schematic view is shown in Figure 1. The test rig consists of the pneumatic cylinder under test and a linear electric cylinder positioned so that their axes are horizontal and their rods face each other. The two rods are connected by means of a universal joint which makes it possible to compensate for any alignment errors in assembly and thus

ensure that force is transmitted axially. The electric cylinder is provided with a ball screw drive and is powered by a brushless rotary motor. Depending on the pressure differential across the pneumatic cylinder piston, the electric cylinder operates with either a driving action or a resistant action.

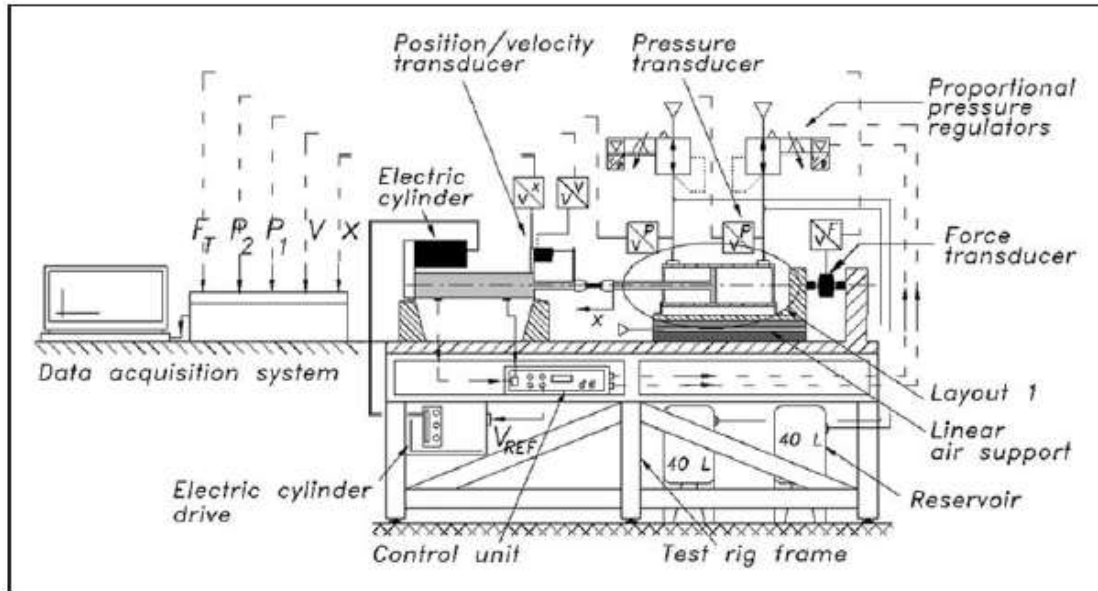


Figure 1: Schematic view of the experimental set-up (basic configuration)

The electric cylinder is secured directly to the test rig frame through L-brackets. The pneumatic cylinder is not connected directly to the frame, but is rigidly retained to the mobile carriage of a linear air guideway. The stationary platform of the guideway is secured to the test rig bed. The pneumatic cylinder/guideway carriage assembly is connected axially, and thus horizontally, to the rig frame via a force transducer. This makes it possible to measure the axial force exchanged between the cylinder under test and the frame, as is necessary in order to determine pneumatic cylinder friction. The force transducer is connected by means of ball joints. As this arrangement ensures that the force transducer is insensitive to dynamic loads, force measurements are not affected by inertia. As the air support has very low friction, moreover, pneumatic cylinder force is correctly and precisely transmitted to the transducer.

An electronic unit drives the electric cylinder and a PI controller provides velocity control using an encoder sensor; the latter is an integral part of the electric cylinder. Pressure in the actuator chambers is regulated by electrically controlled proportional pressure regulators.

The rig is provided with five sensors for measuring piston/rod group displacement and velocity, and pneumatic cylinder chamber pressure and force. Sensor displacement, velocity, pressure and force readings were sent to a low-pass filter to minimise electronic noise. A personal computer was used for data acquisition through an A/D board. Displacement and velocity were measured using a wire-type potentiometer transducer. A series of FGP FN-3030 force transducers ranging from 20 to 500 daN and having an accuracy of 0.1% f.s. was used. FGP FP 210-15-10 strain gauge-based pressure transducers with a nominal resonance frequency of 1 kHz and 0.1% f.s. accuracy were mounted on ISO 6358 standard measurement tubes placed on the test cylinder ports in order to ensure accurate measurements. Camozzi ER200 series proportional pressure regulators (nominal flow rate of about 1000 l/min (ANR)) made it possible to control pressure up to 0.8 MPa. Two 40 litre reservoirs were placed between the regulator outlet and the cylinder ports to reduce pressure oscillation at high flow.

An electric cylinder was chosen, as this made it possible to achieve a larger velocity measurement range, particularly at low running velocities, than conventional systems powered by hydraulic cylinders. Velocity can be controlled in the 0.1 mm/s - 300 mm/s range, as is suitable for testing pneumatic cylinders under actual operating conditions. As the electric cylinder's stroke is 300 mm, pneumatic cylinders of medium stroke can be tested. Thus, tests can be carried out on pneumatic cylinders with a maximum stroke of 250 mm and diameters ranging from 16 to 63 mm.



Figure 2 shows an overall view of the test set-up (Figure 2a) and a detail of assembly (Figure 2b) in the basic configuration (system layout 1). The overall view shows the fixed frame (1), the pneumatic reservoirs (2), the electric cylinder (3), the pneumatic cylinder under test (4) mounted on the carriage of the linear air guideway, the force transducer (5) and the reference signal control unit (6). The detail shows the pneumatic cylinder (4) the linear air guideway (7), the force transducer (5) connecting the cylinder/air guideway carriage assembly to the fixed frame, the pressure transducer (8) and the proportional pressure regulator (9).

### System layout 2

A specific device for measuring the friction force in a pneumatic cylinder piston seal individually. It consists of a special pneumatic cylinder with a double rod (1) and a piston (2) provided with seats for the seals under test (Figure 3); the moving piston-rod group operates within a cylindrical bore (3). The two heads (4) and (5) are sealless and provided with pneumostatic air bearings in order to guide

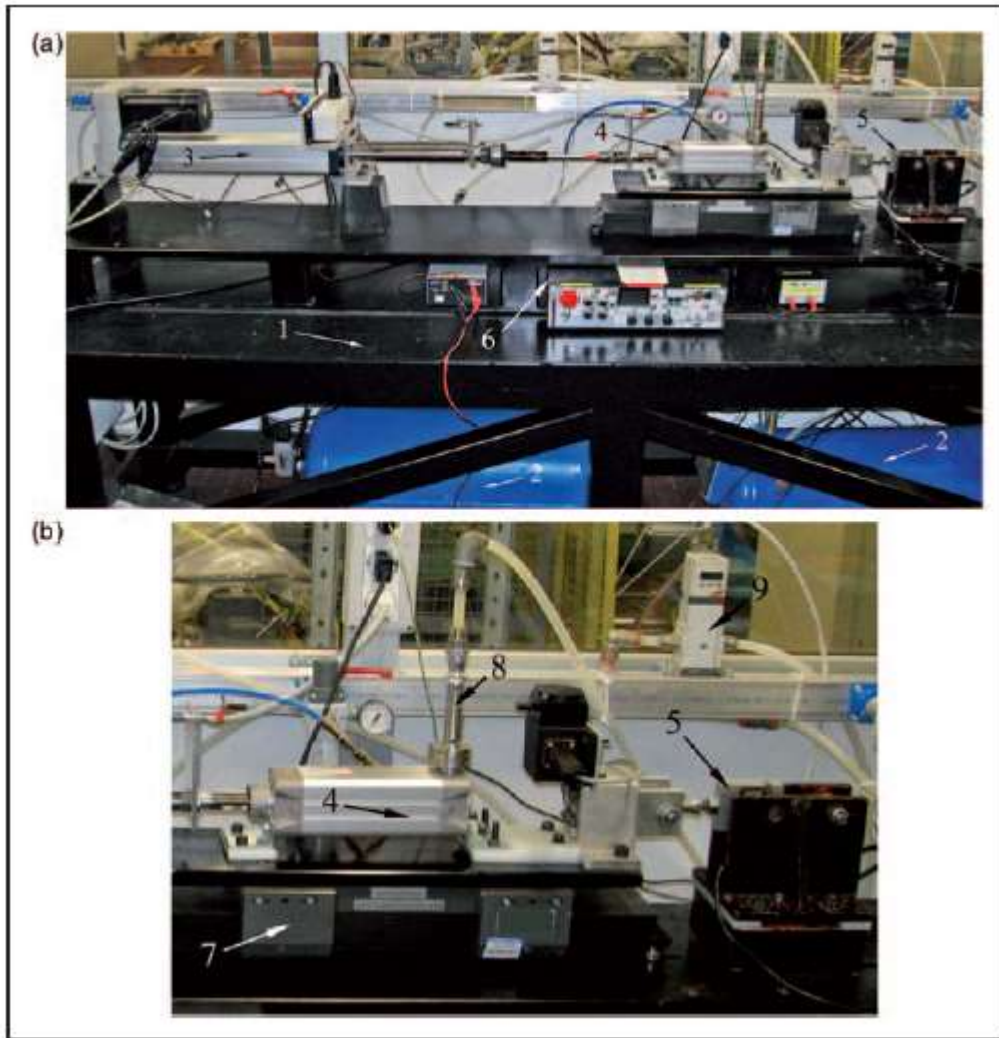


Figure 2: *Test rig for cylinder friction force measurements (system layout 1)*

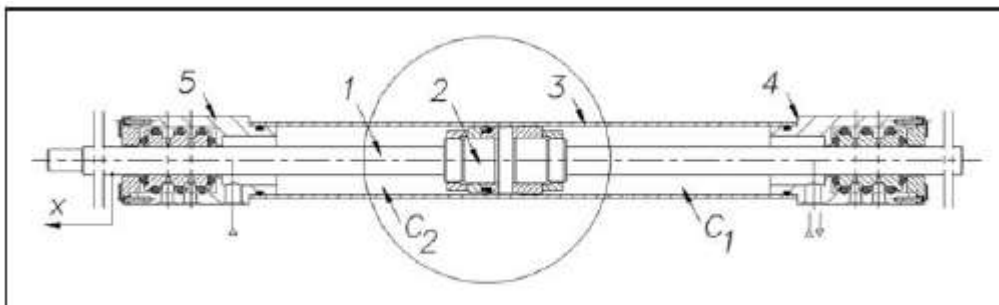


Figure 3: *Schematic view of system layout 2, piston seal friction measurements*

and support the running piston/rod group without additional friction. Depending on test requirements, cylinder chambers C1 and C2 can be pressurised by means of the inlet ports or connected to the atmosphere as described below.

A detail of the group is shown in Figure 4a. The piston rod is symmetrical with respect to the  $y$  axis and can reproduce the mounting seats of standard or special seals for pneumatic cylinders with 50 mm bore. The group can be assembled in three different configurations. In the first configuration, shown in Figure 4a, a single lip seal is installed, as is standard for a single-acting pneumatic cylinder. The lip seal can separate chamber C2, where a pressure load  $P_2$  is applied, from chamber C1 which is commonly connected to the atmosphere; this configuration corresponds to actual working conditions with fluid pressure acting only on the front of the lip. In this way, the seal lip is pressurised against the sliding counterpart, thus ensuring effective sealing and correct behaviour. The seal is installed with a radial pre-load, which also ensures sealing at low pressure loads. The seal under test is mounted in a seat obtained by means of elements (6) and (7) on the central body of the piston (2).

The second configuration features the seal installation shown in Figure 4b. The seal behaves in the same way as in the first configuration, with the lip facing the pressure load  $P_2$  in chamber C2 and atmospheric pressure at the back side of the seal. This is ensured by the radial holes (8) through the piston (2), and the longitudinal hole (9) through the

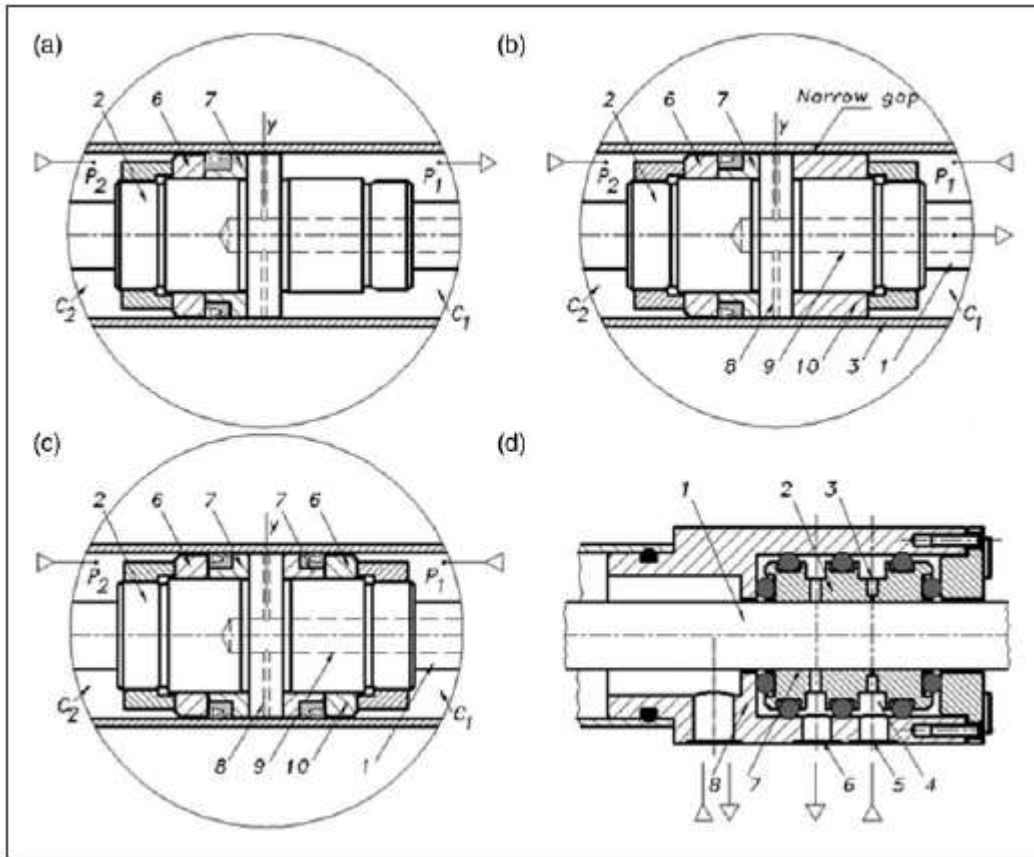


Figure 4: Detail of piston seal friction devices (single and double seal mounting)

piston rod (1) connecting the rear of the seal directly to the atmosphere. If chamber C1 is pressurised with a pressure load  $P_1 = P_2$ , the pressure forces acting on the system are balanced. As result, there is less load on the force sensor and the friction force can be measured directly. With this solution, the force sensor full scale can be as near as possible to the estimated friction force.

The precision ring (10) provides a narrow gap with the cylinder bore (3), thus allowing a very small leakage flow between chamber C1 and the atmosphere through exhaust holes (8) and (9).

The third configuration is shown in Figure 4c. Here, a double lip seal is installed, as is standard in a double-acting pneumatic cylinder. Since the piston body (2) is symmetrical with respect to the y axis, this configuration can be obtained from the

first and second configurations described above, simply by replacing ring (10), in Figure 4b, with rings (6) and (7) which reproduce the seat. Both chambers C1 and C2 can be pressurised at pressure  $P_1$  and  $P_2$  in order to carry out tests and measure friction when a pressure differential across the piston is applied.

Figure 4d shows one of the cylinder heads provided with an air bearing in order to guide and support axial motion of the running piston/rod group. The precision circular gap between the rod (1) and the bearing (2) is pressurised by means of six holes (3) positioned circumferentially; annular chamber (4) collects the air coming from the inlet hole (5). The air in the narrow gap is discharged to the atmosphere directly on the right side of the bearing and by means of the exhaust hole (6); this latter makes it possible to separate the pressure inside each chamber, C1 and C2, and the air bearing supply pressure. Gap (7) machined in the bearing allows a small amount of leakage from the cylinder chambers to the atmosphere, thus separating chamber pressure  $P_1$  or  $P_2$  from air bearing pressure. This leakage flow is discharged to the atmosphere through the common exhaust hole (6). Bearing body (2) is linked to the external housing (8) by rubber O-rings to allow that bearing orientation can change to accommodate rod mounting errors.

The entire system is mounted on a precision guide machined on an intermediate plate which maintains all parts in correct alignment; the system is then connected to the linear air guideway as described for the basic configuration (system layout 1). The photograph in Figure 5 shows fixture 2 assembled without the cylinder bore for clarity; the running double rod (1), the seal-carrying piston (2) in the double seal version, the two heads (4) and (5) with air bearings, the pressure transducers (6), the basic plate (7) and the linear air guideway (8) are pictured.

### System layout 3

This test rig configuration can measure the friction force of a pneumatic cylinder rod seal individually. A special front head with complete rod seal system allowing the seal to operate in actual working conditions was designed and manufactured for this purpose (fixture 3).

The system configuration is shown in Figure 6. This configuration is produced by replacing the

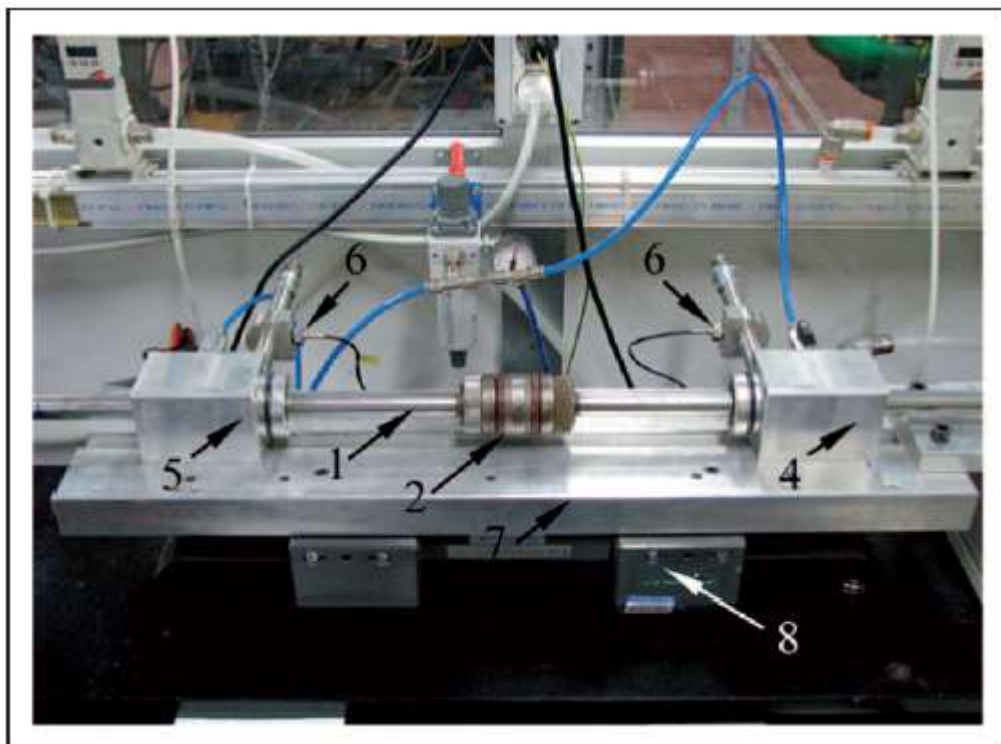


Figure 5: *Piston seal friction measurement fixture*

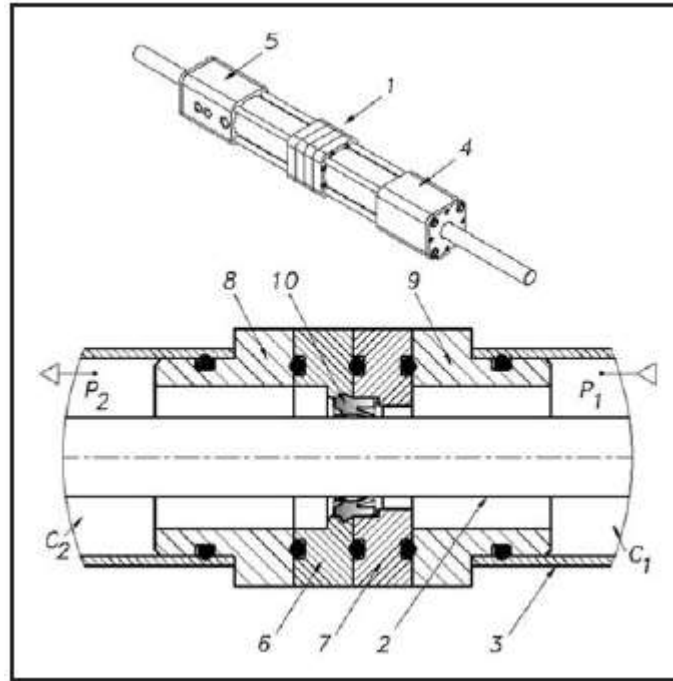


Figure 6: *Detail of the rod seal friction device*

seal-carrying piston and the cylinder bore of fixture 2 with the central heads (1) provided with the seat for the rod seal under test. The single rod (2), connected to the rod of the driven electric cylinder, operates in chambers C1 and C2 inside the cylinder bores (3). The rod slides against the tested seal, and is supported and guided during this motion by the air bearings installed in heads (4) and (5) as in fixture 2 described above. The rod is a commercial type commonly employed in standard pneumatic cylinders: diameter 20 mm, material AISI 304, roughness  $\sim 0.35 \mu\text{m Ra}$ , machining tolerance (0 to  $-0.033 \text{ mm}$ ).

The central head (1) was designed and manufactured to perform as a modular device. Central elements (6) and (7) reproduce the actual mounting seat of the seal under test and can be replaced with others to accommodate different seal geometries and shapes. Side elements (8) and (9) connected to the central units allow the entire head to be joined with a precision coupling to the cylinder bores (3). The seal under test (10)

separates chamber C1 from chamber C2; the former is loaded at pressure  $P_1$  and the latter is generally connected to atmospheric pressure ( $P_2=P_{AMB}$ ). This configuration corresponds to actual working conditions with fluid pressure acting on the front of the lip and the rod scraper directed to the atmosphere.

The photograph in Figure 7 shows fixture 3 fully assembled, with the components described above: the central head (1) carrying the seal under test, the running rod (2), the two lateral air bearings (4, 5), the pressure transducers (6), the basic plates (7) and the linear air guideway (8).

#### System layout 4

This test rig configuration can measure the friction force in pneumatic valve seals individually. A specific device reproducing the behaviour of a standard cartridge/spool system in actual working conditions was designed and manufactured (fixture 4). This is produced by replacing the piston and the bore of fixture 2 with the device shown in Figure 8. Rod (1) is connected on the left side to the driven cylinder, and operates in chambers C1 and C2 inside the cartridge (2). Chamber C2 can be loaded at pressure  $P_2$  by means of the inlet port (3), whereas chamber C1 is





Figure 7: Rod seal friction measurement fixture

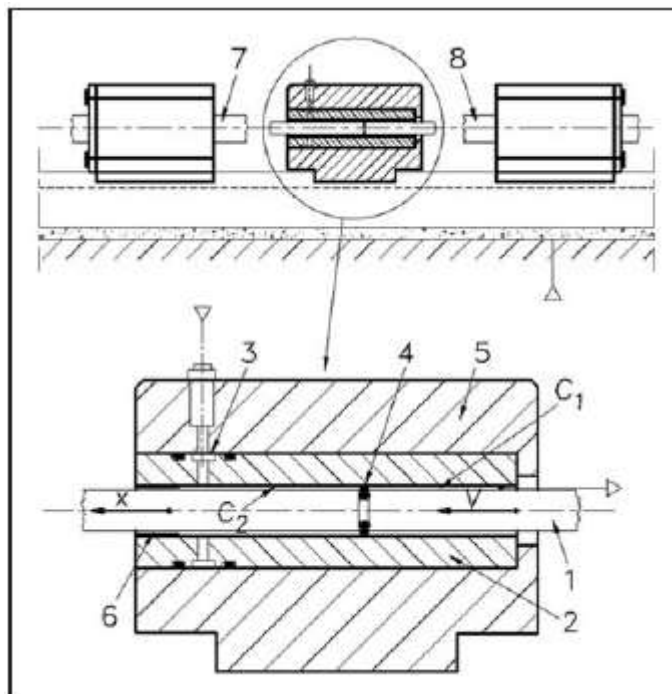


Figure 8: System layout 4, detail of the valve seal friction device

connected to the atmosphere ( $P_1 = P_{AMB}$ ). The seal under test (4) slides against a

bronze cartridge (2) assembled in housing (5); sealing is achieved on one side by the seal under test and on the other side by means of a narrow radial gap (7) provided between the cartridge and the moving rod to minimise leakage. The seal seat is machined on the moving valve rod; this rod has a nominal diameter of 5.20 mm. The cartridge has a nominal inside diameter of 5.35 mm; the narrow gap has a nominal radial value of 20 $\mu$ m.

The linear motion of the moving rod is guided by means of the same linear air bearings used in the layouts described above. To this end, the valve rod (5.35 mm nominal diameter) is connected to two rod parts (8) and (9) (20 mm nominal diameter) which fit into the air bearings.

## **FRICITION FORCE COMPUTATION**

The friction force was computed by applying Newton's force balance equation to the free body diagram for the four different system configurations. The force transducer is connected to the stationary portion of each measurement device, the major advantage of this approach being that the measurement is not influenced by the inertia acting on the moving parts.

For the basic configuration of the system (layout 1), the balance equation of the forces acting on the cylinder bore/air carriage assembly, while the cylinder piston is moving at constant velocity  $V$ , gives:

$$P_1A_1 - P_2A_2 - (F_S + F_R + F_{PG}) - F_{FT} - F_{AG} = 0$$

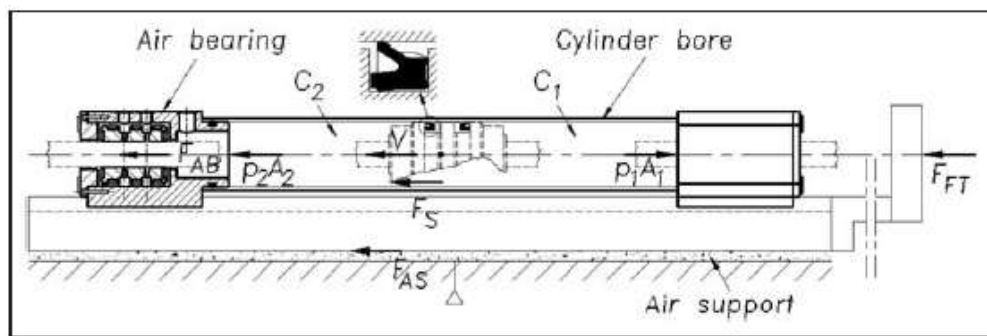
where  $P_1$  and  $P_2$  are the pressures in the rear and front chambers respectively,  $A_1$  and  $A_2$  are the cylinder cross-sectional areas of the rear and front chambers respectively,  $F_{FT}$  is the force measured by the force transducer,  $F_S$  is the piston seal friction force,  $F_R$  is the rod seal friction force,  $F_{PG}$  is the friction force due to the piston guide

system (slide ring and rod guide) and  $F_{AG}$  is the friction force exerted by the air guideway. The overall friction force, i.e., the sum of friction at the piston seals, at the rod seal and at the cylinder guiding systems, can thus be expressed as:

$$F = P_1 A_1 - P_2 A_2 - F_{FT} - F_{AG}$$

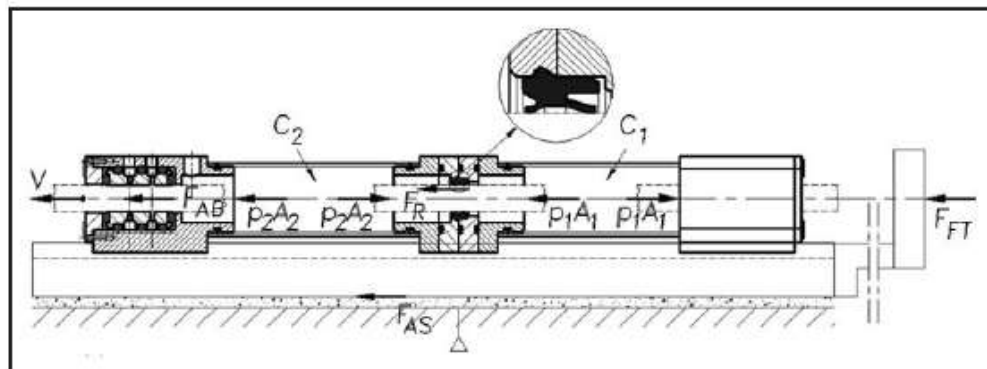
Table 1: Free body diagram of the bore/air guideway assembly (layout 2 and 3)

System layout 2 – cylinder piston seal ( $A_1 = A_2 = A$ : cross-sectional area of the chambers)



Double seal assembly  
 $F_S = (P_1 - P_2)A - F_{FT}$   
 Single seal assembly  
 $F_S = -F_{FT}$

System layout 3 – cylinder rod seal



$F_S = -F_{FT}$

Linear air guideway friction  $F_{AG}$  is negligible.

For system layout 2, the forces acting on the bore/air guideway assembly are shown in Table 1; the piston/rod group is moving at constant velocity  $V$ . Diagram can be applied both to double lip seal and single lip seal assemblies, which are typical of standard double- and single-acting cylinders respectively. The force balance equation gives:

$$F_S = P_1 A_1 - P_2 A_2 - F_{FT} - F_{AG} - F_{AB}$$

where  $A_1 = A_2$  as the system features a double rod cylinder,  $F_S$  is the piston seal friction force and  $F_{AB}$  is the friction force due to both piston/rod group air bearings.

Forces  $F_{AB}$  and  $F_{AG}$  are negligible.

When a single piston seal is installed, using the configuration of Fig. 4a, the front chamber is pressurised at  $P_2$  and the rear chamber is connected to the atmosphere by means of the exhaust port ( $P_1 = P_{AMB}$ ). The single piston can be installed using the configuration shown in Figure 4b; the front chamber C1 and rear chamber C2 are pressurised at  $P_2$  and  $P_1$  respectively. Thanks to the narrow gap and the axial hole inside the rod, atmospheric pressure is ensured at the back side of the lip seal. In this case, supplying the chambers at the same pressure level ( $P_2 = P_1$ ) creates a balance of acting pressure forces, and friction force can be measured directly by means of the force transducer; in fact, neglecting air bearing and air support friction, the balance equation gives:

$$F_S = -F_{FT}$$

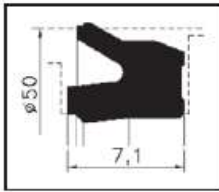
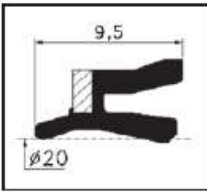
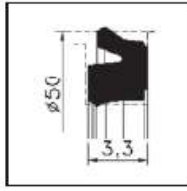
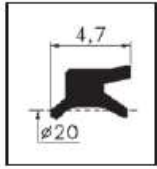
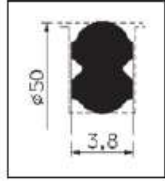
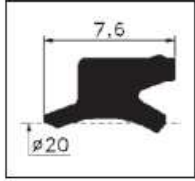
For system layout 3 with cylinder rod seal, the forces acting on the central head/air guideway assembly are shown in Table 1; the rod is moving at constant velocity  $V$ . This assembly configuration corresponds to actual working conditions with compressed air acting only on one side of the rod seal and with atmospheric pressure on the rod scraper ( $P_2 = P_{AMB}$ ). As in the previous case, the cylinder cross-sectional areas of the rear and front chambers are identical ( $A_1 = A_2$ ),  $F_R$  is the rod seal friction force; the meaning of the other symbols remains the same. Neglecting  $F_{AB}$  and  $F_{AG}$  and taking into account that the pressure forces in each chamber C1 and C2 are self-balanced, the equilibrium becomes:

$$F_R = -F_{FT}$$

Similar considerations can be applied to system layout 4, shown in Figure 8, for calculating the friction force for an individual valve seal.

Fiction force computation is summarised in Table 1.

Table 2: Main characteristics of tested cylinders and seals

Cylinder group	Bore/rod material		Piston seals		Rod seals	
	Cylinder bore	Rod	Material	Cross-section	Material	Cross-section
A	Anodised aluminium	High alloy steel	HNBR		NBR	
B	Anodised aluminium	Chromium plated steel	Poly-urethane		NBR	
C	Anodised aluminium	Chromium plated steel	NBR		NBR	
A, B, C	Ra ≅ 0.6 μm t ≅ (0, +0.2)	Ra ≅ 0.35 μm t ≅ (0, -0.033)	Grease type: synthetic, with active PTFE components t = machining tolerances; dimensions in mm.			

## MATERIAL AND TEST CONDITIONS

Tests were carried out on complete commercial ISO 15551 double-acting pneumatic cylinders from three different manufacturers but with similar characteristics and technical specifications. All featured 50 mm bore, 20 mm rod diameter, 160 mm, and were grease lubricated for life cylinders. Each group of cylinders (A, B, C) consists of at least three samples of the same type. Table 2 shows details of main cylinder characteristics and specifications; the groups of cylinders differed chiefly in the

geometry of the internal seals. A typical dimension of the cross section is shown for each seal.

Two types of test conditions with different pressures in the pneumatic cylinder chambers were used in order to cover a range of conditions reproducing actual operating conditions. In condition 1, relative pressure in the rear chamber  $C_1$  is in the  $p_1 = 0 \div 6$  bar range and pressure in the front chamber  $C_2$  is  $p_2 = 0$  bar. In condition 2, relative pressure in the front chamber  $C_2$  is in the  $p_2 = 0 \div 6$  bar range and pressure in the rear chamber  $C_1$  is  $p_1 = 0$  bar. Tests were carried out for both directions of the piston/rod assembly, with a velocity range  $V \cong 0.1 \div 300$  mm/s. Velocity was considered positive during pneumatic cylinder extension (outstroke) and negative during retraction (instroke). Chamber 1 behaves either as a driving chamber, when velocity is positive, or as a resistant chamber, when velocity is negative. The converse is true for chamber 2. Test conditions are summarised in Table 3.

At least three outstrokes and instrokes were performed for each measurement point, with at least nine different constant velocity values in both positive and negative directions for each load pressure condition. The data acquisition program takes into account zero settings and calculates friction force by processing data using the balance equations described above.

## **FRICION TEST RESULTS**

Performance was analyzed as regards the macroscopic tribological aspects of the actuators under test. Specifically, analyses addressed behaviour as a function of operating pressure in the chambers, rod actuation velocity, direction of velocity and seal type and geometry. The choice of these parameters was based on the necessity of separate the contribution of single seals from the overall friction of the actuator

considered as a black-box. The variations in surface roughness, machining tolerances and seal/counterpart

Table 3: *Test conditions*

Test condition	$p_1$ (bar)	$p_2$ (bar)	$V$ (mm/s)
1	0, 2, 4, 6	0	$\pm(0.1 \text{ to } 300)$
2	0	0, 2, 4, 6	$\pm(0.1 \text{ to } 300)$

materials between cylinder groups A, B, and C are too small for the effects to be detected through comparative analyses of the friction forces measured in macroscopic tests such as those carried out in this investigation. The measured friction force includes also the contributions of piston slide ring and rod guide. Results given below are average values obtained by repeating measurements at least three times for each test condition and each of the cylinder samples in each group under test.

The analysis of the experimental results will highlight different behaviours and phenomena: the friction dependence on sliding direction due to binding or non-binding action of the seal lip, the effect of chamber pressure connected to the seal geometry (pressure with driving or resistant action, lip seal or double-lobed seal), the effect of rod seal geometry with respect to the pressure in the front chamber. In particular the obtained results will be analysed and explained on the base of phenomena suggested above in order to evaluate the individual behaviour of the sliding seals of the actuators under test.

Figures 9 and 10 show friction force versus velocity and operating pressure (test

conditions 1 and 2); the results refer to group A cylinders with a double lip seal on the piston and a single lip seal on the rod. From the quality standpoint, behaviour is very similar to that found for group B cylinders, which feature similar sealing arrangements. As the curves indicate, friction force increases along with velocity and chamber pressures. Friction force is higher when the chamber is operating with a resistant action (quadrant III in Figure 9 and quadrant I in Figure 10 ) than when the same chamber is operating as a driving chamber (quadrant I in Figure 9 and quadrant III in Figure 10 ).

This fact is attributable to the lip geometry of the seals, which is such that friction force is not symmetrical with respect to the direction of velocity. For the piston seals in particular, the lip exerts a “binding” action on the barrel when it is oriented in the direction of velocity, and a “non-binding” action in the opposite case. As the seal consists of a deformable elastomer, the higher the fluid pressure, the clearer the effect will be.

This behaviour is particularly apparent in Figure 9, as this figure refers to the test condition (test condition 1) in which only one seal, viz., piston seal S1, is pressurised. Depending on lip orientation, seal S1 does not bind in the positive direction of motion (quadrant I), and binds in the negative direction (the friction force is higher in this latter condition). When there is no fluid pressure, by contrast, friction behaviour is practically symmetrical in both directions of motion. In addition, friction force is also non-symmetrical when both chambers are operating in the same mode (e.g., chambers 1 and 2 in driving operation ), given that the system is geometrically non-symmetric because the pressurised rod seal causes friction force levels that are higher when chamber 2 is pressurised.

The graph in Figure 11 shows the performance of group C cylinders for the test



condition in which both chambers 1 and 2 are pressurised (separately) and fluid pressure provides a driving action ( $p_{1D}$ ,  $p_{2D}$ ). For driving chamber 1, the only seal acted on by fluid pressure is the piston seal; unlike the previous cases, this seal is a double-lobed unit rather than a lip seal. As a result, the friction curves differ much less as operating pressure varies than in the previous cases. Friction is still non-symmetric for the two directions of velocity, though to a lesser extent: this behaviour is due to the change in the direction of friction which, by causing local seal deformation, creates strains that are normal and tangential to contact which depend on the direction of motion. For driving chamber 2, the pressure also acts on the lip-type rod seal. Compared to the previous case, in which the lip seal was not involved, there is a greater difference between the friction curves under the action of operating pressure in the chamber.

Performance for group A actuators when both chambers 1 and 2 operate as driving chambers is compared in Figure 12; friction forces for the two cases are shown in quadrant I. The graph confirms that actuator friction force, in the case where fluid pressure acts as a driving pressure, is higher in chamber 2 than

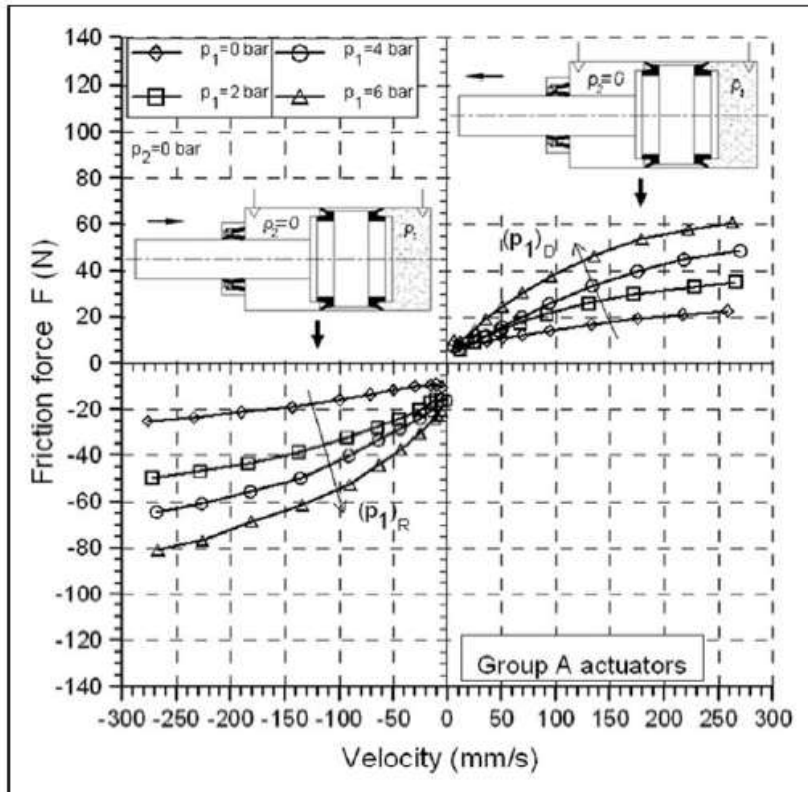


Figure 9: Friction force, load condition 1 ( $p_2=0$  bar,  $p_1$  variable)

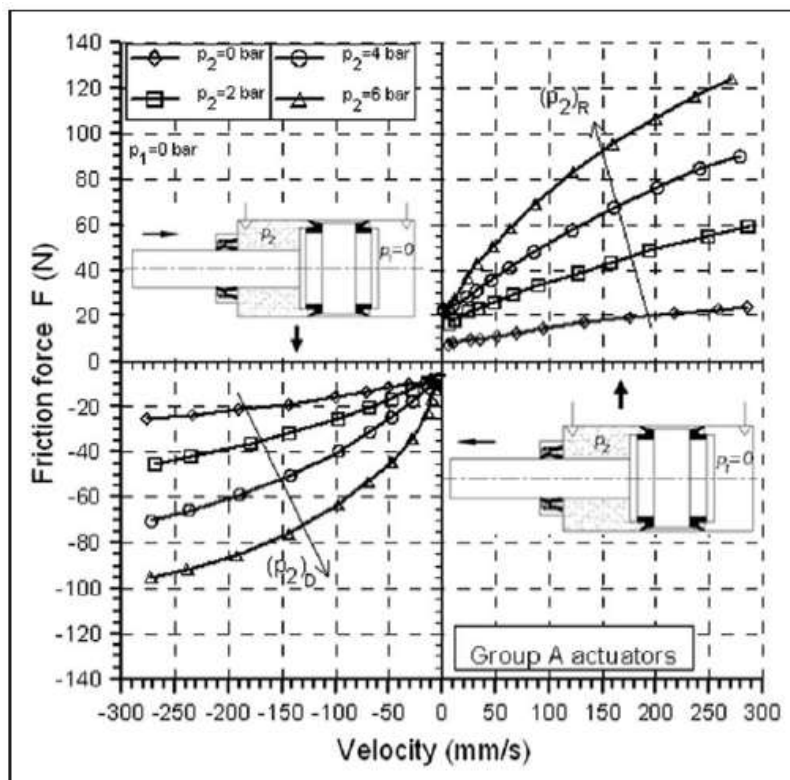


Figure 10: Friction force, load condition 2 ( $p_1=0$  bar,  $p_2$  variable)

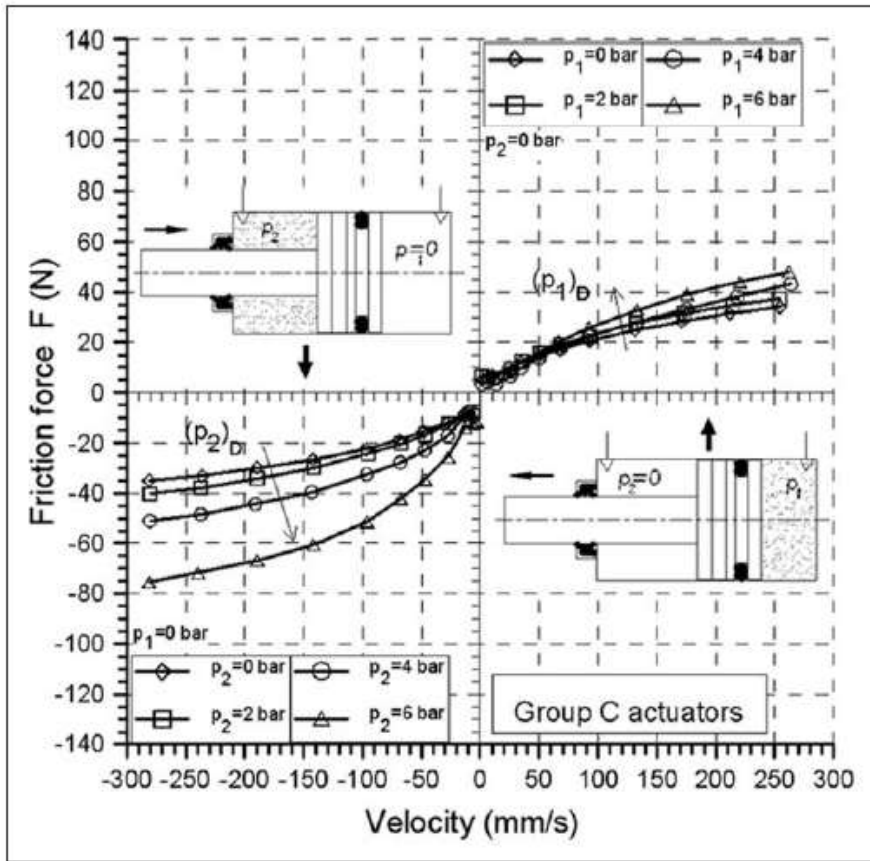


Figure 11: Friction force, load condition 1 and 2 (driving chambers)

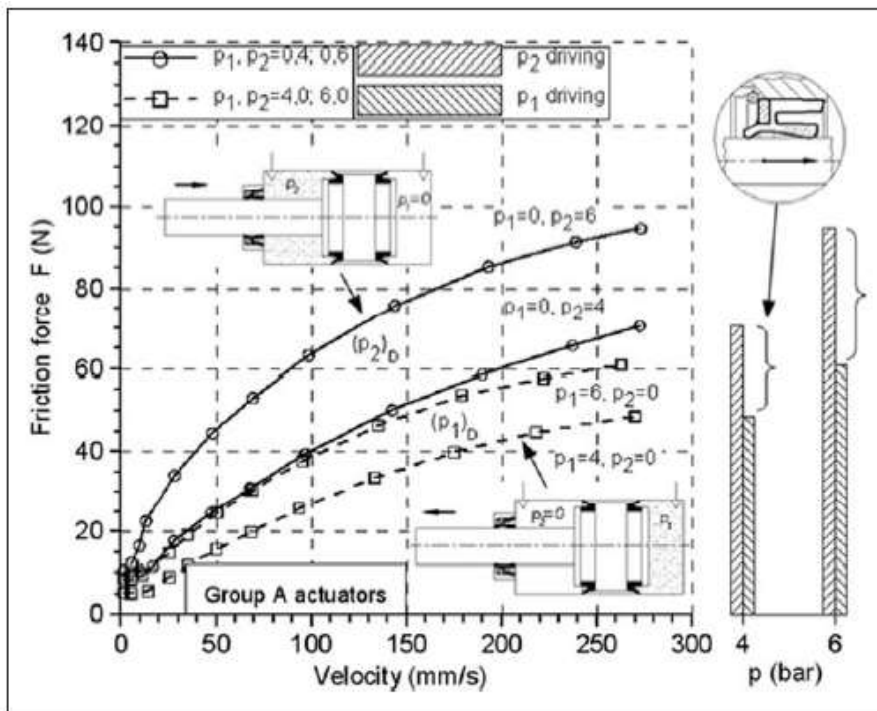


Figure 12: Friction force comparison (driving chambers)

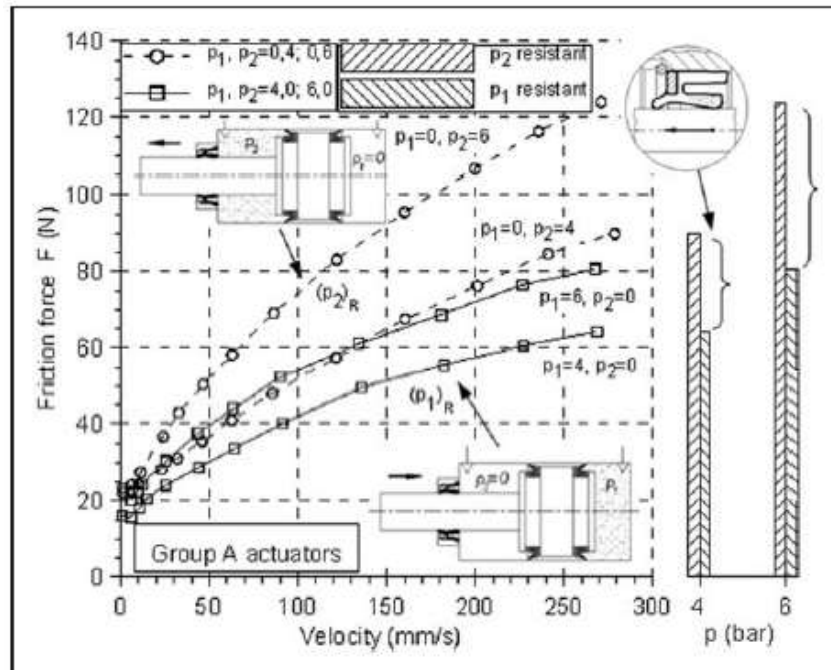


Figure 13: Friction force comparison (resistant chambers)

in chamber 1. The bar chart on the right, which shows maximum velocity achieved during testing ( $\approx 270$  mm/s), highlights the increase in this difference between friction forces as operating pressure in the chambers rises.

Figure 13 shows friction forces in group A actuators, comparing the behaviour of chamber 2 and chamber 1 when they operate separately as resistant chambers. The directional behaviour of seal friction force and the presence of the rod seal result in a higher friction force when chamber 2 is the resistant chamber.

Aside from the friction force levels, considerations similar to those indicated above also apply to group B and C actuators.

Analyzing the actuator's overall friction force, i.e., that for the operation of the entire system, makes it possible to identify the local behaviour of the individual seals, with the differences in operation that occur when cross-sectional geometry, seal type (piston or rod) and direction of sliding motion are varied. To this end, the contributions made by the individual seals must be separated from the actuator's

overall friction force.

We will first address the case in which the chambers operate as driving chambers.

Here, the overall friction force is:

$$(F)_{p_2}^D = (F_{S1})_0^B + (F_{S2})_{p_2}^{NB} + (F_{RL})_{p_2}^{NB} + (F_{RS})^B \quad (p_2 \text{ driving, v-}) \quad (1)$$

$$(F)_{p_1}^D = (F_{S1})_{p_1}^{NB} + (F_{S2})_0^B + (F_{RL})_0^B + (F_{RS})^{NB} \quad (p_1 \text{ driving, v+}) \quad (2)$$

The meaning of the subscripts and superscripts in these expressions is as follows:  $0$  – seal in unpressurised conditions ( $p = 0$  bar relative);  $B$  – seal in binding operating condition;  $NB$  – seal in non-binding operating condition;  $p_1, p_2$  seal pressurised with pressure acting in chamber  $C_1$  or  $C_2$  respectively.  $(F)_{p_2}^D$  thus denotes the cylinder's overall friction force when chamber  $C_2$ , pressurised at  $p_2$ , operates as a driving chamber. Similarly,  $(F)_{p_1}^D$  denotes the overall friction force with pressure  $p_1$  in driving operation. The contributions to overall friction by the piston seal ( $S_1, S_2$ ), rod seal lip (RL) and rod seal scraper (RS) are shown to the right of the equal sign; pressurisation condition and direction of motion acting on the individual seal are taken into account in evaluating each contribution. The contribution made by the cylinder guide elements is not indicated, as it is simplified in the subsequent steps.

Subtracting member by member the expressions (1) and (2) with the same pressure in the chambers ( $p_1 = p_2 = p$ ) and bearing in mind that  $S_1$  and  $S_2$  are geometrically the same seal, we have:

$$\left[ (F)_{p_2} - (F)_{p_1} \right]^D = (F_{RL})_{p_2}^{NB} - (F_{RL})_0^B + \left[ (F_{RS})^B - (F_{RS})^{NB} \right] \quad (3)$$

As tests with no fluid pressure indicated that friction force does not depend on the direction of motion, we can rule out an asymmetric behaviour of the rod scraper

( $F_{RS}^B = F_{RS}^{NB}$ ) and the rod seal lip ( $(F_{RL})_0^B = (F_{RL})_0^{NB}$ ). At this point, expression (3)

can be rewritten as follows:

$$(\Delta F_{2-1})^D = [(F)_{p_2} - (F)_{p_1}]^D = (F_{RL})_{p_2}^{NB} - (F_{RL})_0^{NB} \quad (3')$$

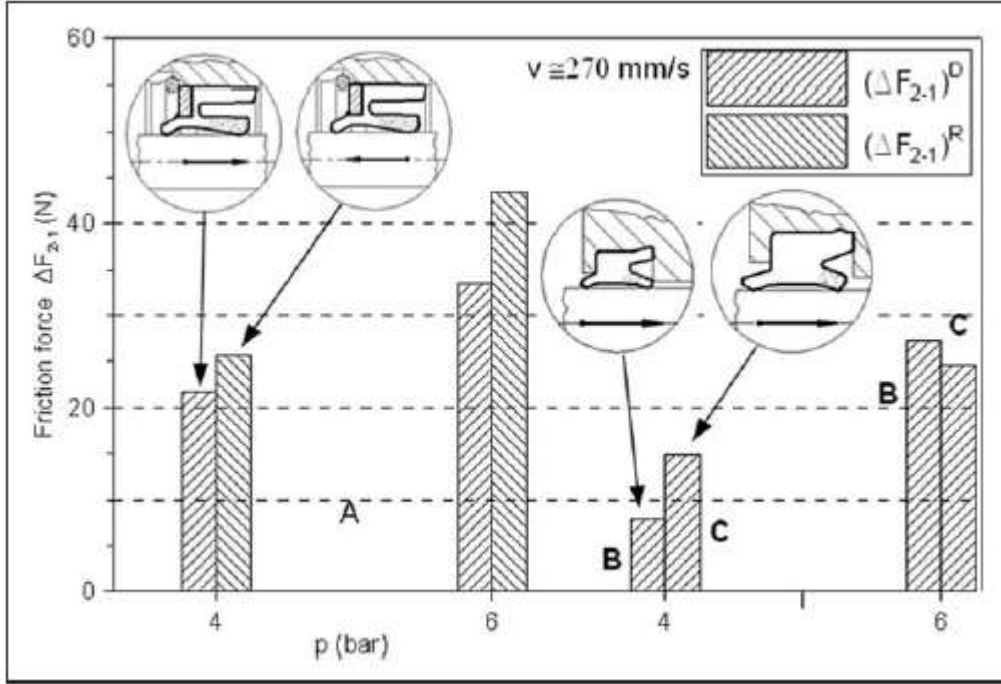


Figure 14: Friction force comparison (driving/resistant chambers)

In other words, the difference in overall actuator friction force when chamber 2 and chamber 1 operate independently as driving chambers is due to the contribution of the pressurised rod seal in “non-binding” operating conditions, less the friction contribution of the same seal on assembly.

For the case in which the chambers operate as resistant chambers and bearing the foregoing considerations in mind, we obtain the following expression:

$$(\Delta F_{2-1})^R = [(F)_{p_2} - (F)_{p_1}]^R = (F_{RL})_{p_2}^B - (F_{RL})_0^B \quad (4)$$

Here, by contrast with (3'), the contribution of the rod seal is in “binding” operating conditions.

The results of expressions (3') and (4) are compared in the bar chart in Figure 14, which shows the difference in friction force  $(\Delta F_{2,1})^D$  between chambers 2 and 1 in

driving operation (eqn. (3')) and the difference in friction force  $(\Delta F_{2,1})^R$  between chambers 2 and 1 in resistant operation (eqn. (4)). In the second case, where the rod seal is in “binding” operation, the result in terms of friction is larger than in the first case with “non-binding” seal; the difference increases along with operating pressure. By way of comparison, the figure also shows the result obtained with equation (3') for group B and C actuators with the seal in “non-binding” conditions. Seal A exhibits a higher friction force than seals B and C, for any given operating pressure and direction of relative motion. For seal B, moreover, friction is more dependent on increases in operating pressure than for seals A and C. In the case of seal A, this behaviour is due to the metal ring provided to stiffen the seal structure, whereas for seal C, the greater structural stiffness and strength are inherent to the cross-sectional shape.

Turning to the case in which chamber 1 operates, separately, both as a driving chamber and as a resistant chamber and taking the foregoing considerations into account, we have:

$$(\Delta F_1)^{R,D} = [(F)_{p_1}^R - (F)_{p_1}^D] = (F_{S1})_{p_1}^B - (F_{S1})_{p_1}^{NB} \quad (p_1 \text{ resistant/driving}) \quad (5)$$

In other words, the result of subtracting the actuator friction force when chamber 1 operates as a driving chamber from the actuator friction force when this chamber is resistant gives the difference between the friction exerted by the pressurised piston seal in “binding” operation and that exerted in “non-binding” operation. This difference thus highlights the asymmetry exhibited by piston seal friction in the two directions of motion. For purposes of comparison, the bar chart in Figure 15 shows the results of this difference in friction force for the actuators in question; the force is that at the maximum velocity reached during testing for different pressures. In all cases, it can be seen that the difference in friction force is lower during no-load

operation, i.e., with no pressure, and increases along with air operating pressure. This increase is less than proportional, with a tendency to flatten out at higher pressures. The increase in fluid pressure, by stiffening the seal's structure and reducing its flexibility, makes the geometry less sensitive to variations in deformation caused by sliding friction load reversal. The piston seal on group C actuators, which is not a lip type, is the least sensitive to differences in friction behaviour depending on direction of motion. The differences in friction force are lower than for cases A and B with a lip seal on the piston. Because of the seal's rounded, compact shape and lower radial

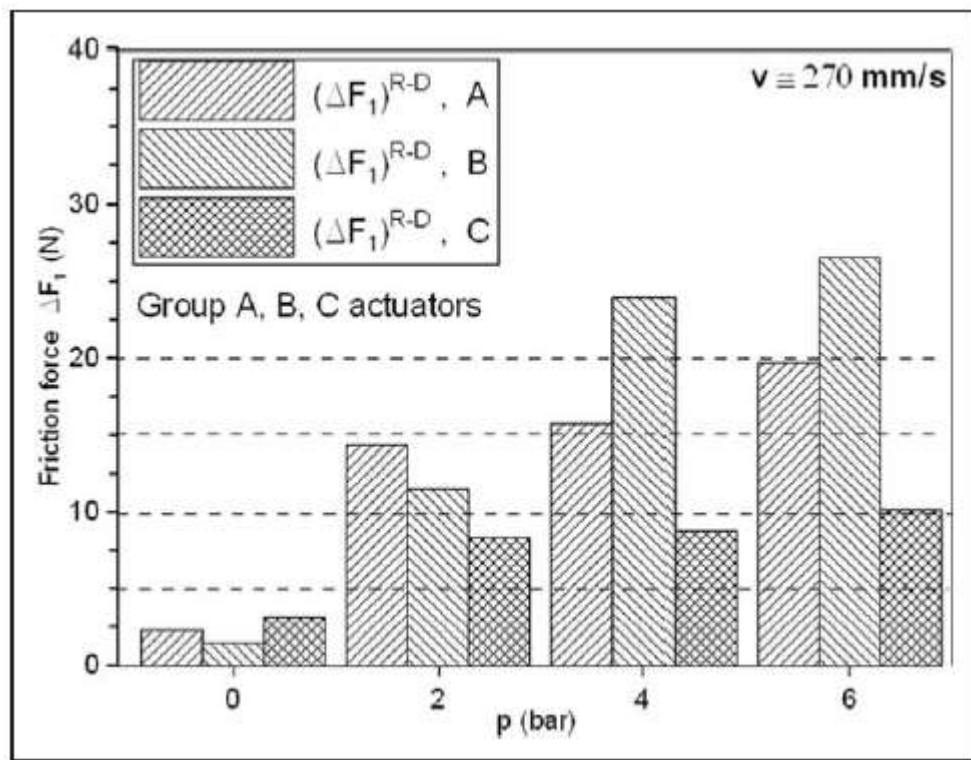


Figure 15: Friction force comparison (driving/resistant chambers)

flexibility, moreover, the tendency of the difference in friction force to flatten out as operating pressure increases is more marked in case C than in cases A and B; in other words, in case C, the gap between “binding” and “non-binding” behaviour is less sensitive to increases in operating pressure than in cases A and B.



## CONCLUSIONS

A new test rig for measuring friction in pneumatic components and seals was designed and manufactured. The test rig was conceived as a modular system that can be adapted to different configurations in order to measure both the overall friction force in pneumatic cylinders and valves as a whole, and the contribution to friction of individual sliding seals. To this end, special equipment reproducing the behaviour of a piston-bore system or a front head-rod system were designed.

Friction force tests on commercial pneumatic cylinders, considered as a whole, were performed and presented. Different operating conditions were established, with varying pressure differentials across the chambers and instroke/outstroke velocities. This made it possible to investigate the system with the cylinder chambers behaving both as driving and resistant chambers. As regards the direction of velocity, friction behaviour was found to be a non-symmetric in different directions of velocity and front and rear chamber operating modes. The lip seals in particular exhibited behaviour which is highly dependent on direction of motion, leading to a non-binding action with lower friction force, or a binding action with higher friction force. This behaviour depends on operating pressure in the actuator chambers; when there is no pressure load in the chambers, friction is symmetrical in both directions of velocity. Non-lip type seals with double-lobe geometry show less variation in friction force as fluid pressure increases and greater friction force symmetry with respect to the direction of velocity.

An analysis of the overall friction force measured on the complete actuator made it possible to separate the contributions of the sliding elements, and thus evaluate the local behaviour of individual seals. In particular, different types of rod lip seal were

found to exhibit differences in behaviour as operating conditions were varied. In all cases analyzed, friction force showed a more or less marked dependence on direction of motion; for any given lip type, tests showed variations in friction force as a function of operating pressure that were highly dependent on cross-sectional stiffness and shape. For the piston seal, the double-lobe types showed smaller differences between binding and non-binding behaviour, with less sensitivity to rising pressure.

Though the analyses on individual seals using measurements carried out on complete actuators made it possible to evaluate only the relative behaviour in different operating conditions (e.g., pressurised rod seal compared to the same seal without pressure load), the graphs and results permit significant comparisons both between the seals of the same actuator (piston and rod), and between the seals of actuators from different manufacturers. The results can provide guidance in making decisions both at the design stage and during component selection on the part of the user. To obtain more detailed results under specific test conditions, it will be necessary to carry out tests on individual components using dedicated equipment such as that designed for this investigation.

## **ACKNOWLEDGEMENTS**

The authors wish to acknowledge the support of the European Commission and project partners in KRISTAL, Knowledge-based Radical Innovation Surfacing for Tribology and Advanced Lubrication (EU Project Reference NMP3-CT-2005-515837). The authors would like to thank Dr. F.S. Camarda for his help.

## **REFERENCES**

- 1 Belforte, G., D'Alfio, N. and Raparelli, T. Experimental analysis of friction

- forces in pneumatic cylinders. *The Journal of Fluid Control*, 1989, **78**, 42-60.
- 2 Schroeder, L.E. and Singh, R. Experimental study of friction in a pneumatic actuator at constant velocity. *J. Dyn Sys., Meas., Control*, 1996, **115**, 575-577.
  - 3 Eschmann, R. Misura dell'attrito di guarnizioni in cilindri pneumatici. *Fluid*, 1993, **349**, 115-119.
  - 4 Ellman, A.U., Koivula, T.S. and Vilenius M.J. Hydraulic cylinder seal friction – Comparison of two seal designs. In Proceedings of the 15<sup>th</sup> International Conference on *Fluid Sealing*, Maastricht, The Netherlands, 1997, pp. 133-142.
  - 5 Kazama, T. and Fujiwara, M. Experiment on frictional characteristics of pneumatic cylinders. In Proceedings of the 4<sup>th</sup> JHPS International Symposium on *Fluid Power*, Tokio, Japan, 1999, pp. 453-458.
  - 6 Belforte, G., Mattiazzo, G., Mauro, S. and Tokashiki, L.R. Measurement of friction force in pneumatic cylinders. *Tribotest Journal*, 2003, **10**, 33-48.
  - 7 Muller, H.K., Messner, N. PTFE – Seals for reciprocating rods. In Proceedings of the 9<sup>th</sup> International Conference on *Fluid Sealing*, Noordwijkerhout, The Netherlands, 1981, pp.389-402.
  - 8 Prokop, H. J., Muller, H.K. Film thickness, contact pressure and friction of PTFE rod seals. In Proceedings of the 12<sup>th</sup> International Conference on *Fluid Sealing*, Brighton, UK, 1989, pp.147-163.
  - 9 Belforte, G., Raparelli, T. and Velardocchia, M. Study of the behavior of lip seals in pneumatic actuators. *Lubr. Eng.*, 1993, **49**, 775-780.
  - 10 Belforte, G., Raparelli, T. and Velardocchia, M. Effect of mounting tolerances on pneumatic cylinder lip seal friction forces. *Lubr. Eng.*, 1994, **50**, 841-845.
  - 11 Raparelli, T., Manuello Bertetto, A. and Mazza, L. Experimental and numerical study of friction in an elastomeric seal for pneumatic cylinders. *Trib. Int.*, 1997,

**30**, 547-552.

- 12 Wassink, D.B., Lenss, V.G., Levitt, J.A., Ludema, K.C. and Samus, M.A. Friction dynamics in sliding lip seals. In Proceedings of the 47<sup>th</sup> National Conference on *Fluid Power*, Chicago, Illinois, USA, 1996, pp. 205-211.
- 13 Wassink, D.B., Lenss, V.G., Levitt, J.A. and Ludema, K.C. Physically based modelling of reciprocating lip seal friction. *J. Tribol.*, 2001, **123**, 404-412.
- 14 Jansen, N., Haas, W., Lambert, M. Tests on contaminations of wipers fro linear guidance. In Proceedings of the 17<sup>th</sup> International Conference on *Fluid Sealing*, York, UK, 2003, pp.217-228.
- 15 Horl, L., Haas, W., Nisler, U. A comparison of test methods for hydraulic rod seals. *Sealing Tech.*, 2009, **12**, 8-13.
- 16 Calvert, C., Tirovic, M. and Stolarski, T. Design and Development of an Elastomer-based Pneumatic Seal using Finite Element Analysis. *Proc. IMechE, Part J: J. Engineering Tribology*, 2002, **216**(J3), 127-138.
- 17 Belforte, G., Manuello Bertetto, A. and Mazza, L., Optimization of the Cross-Section of an Elastomeric Seal for Pneumatic Cylinders. *J.Tribol.*, 2006, **128**, 406-413.
- 18 Helduser, S. and Muth, A. Dynamic friction measurement method evaluated by means of cylinders and valves. In Proceedings of the 3<sup>rd</sup> JHPS International Symposium on *Fluid Power*, Jokohama, Japan, 1996, pp. 271-276.
- 19 Fujii, Y. Method for measuring transient friction coefficients for rubber wiper blades on glass surface. *Trib. Int.*, 2008, **41**, 17-23.

## NOTATION

$C_1$ , rear chamber

$F_{AS}$ , air support friction force

$C_2$ , front chamber	$F_{AB}$ , piston air bearing friction
$A_1$ , rear chamber cross-sectional area	$(F)_{p_2}^D$ , $(F)_{p_1}^D$ , overall friction force, pressure load $p_2$ or $p_1$ , driving
$A_2$ , front chamber cross-sectional area	$(F_{S_2})_{p_2}^{NB}$ , $(F_{S_1})_{p_1}^{NB}$ , $S_2$ or $S_1$ piston seal friction, pressurised seal, “non-binding” lip
$P_1$ , rear chamber pressure	$(F_{S_1})_{p_1}^B$ , $S_1$ piston seal friction, pressurised seal, “binding” lip
$P_2$ , front chamber pressure	$(F_{S_1})_0^B$ , $(F_{S_2})_0^B$ , $S_1$ or $S_2$ piston seal friction, zero pressure, “binding” lip
$F$ , overall friction force	$(F_{RL})_{p_2}^{NB}$ , rod seal lip friction, pressurised seal, “non-binding” lip
$F_{FT}$ , force transducer	$(F_{RL})_0^B$ , rod seal lip friction, zero pressure, “binding” lip
$F_S$ , piston seal friction force	$(F_{RS})^B$ , $(F_{RS})^{NB}$ , rod seal scraper friction, “binding” or “non-binding” scraper respectively
$F_R$ , rod seal friction force	$(\Delta F_{2-1})^D$ , overall friction force difference, $p_2$ and $p_1$ driving pressure
$F_{PG}$ , piston guide system friction force	$(\Delta F_{2-1})^R$ , overall friction force difference, $p_2$ and $p_1$ resistant pressure